Clarifying the Roles of Greenhouse Gases and ENSO in Recent Global Warming through Their Prediction Performance

UMBERTO TRIACCA

Department of Computer Engineering, Computer Science and Mathematics, University of L'Aquila, L'Aquila, Italy

ANTONELLO PASINI AND ALESSANDRO ATTANASIO

National Research Council (CNR), Institute of Atmospheric Pollution Research, Monterotondo Stazione, Rome, Italy

ALESSANDRO GIOVANNELLI

Department of Economics and Finance, University of Tor Vergata, Rome, Italy

MARCO LIPPI

Einaudi Institute for Economics and Finance, Rome, Italy

(Manuscript received 17 December 2013, in final form 24 July 2014)

ABSTRACT

It is well known that natural external forcings and decadal-to-millennial variability drove changes in the climate system throughout the Holocene. Regarding recent times, attribution studies have shown that greenhouse gases (GHGs) determined the trend of temperature (T) in the last half century, while circulation patterns contributed to modify its interannual, decadal, or multidecadal behavior over this period. Here temperature predictions based on vector autoregressive models (VARs) have been used to study the influence of GHGs and El Niño–Southern Oscillation (ENSO) on recent temperature behavior. It is found that in the last decades of steep temperature increase, ENSO shows just a very short-range influence on T, while GHGs are dominant for each forecast horizon. Conversely and quite surprisingly, in the previous quasi-stationary period the influences of GHGs and ENSO are comparable, even at longer range. Therefore, if the recent hiatus in global temperatures should persist into the near future, an enhancement of the role of ENSO can be expected. Finally, the predictive ability of GHGs is more evident in the Southern Hemisphere, where the temperature series is smoother.

1. Introduction

Many studies have investigated the causes of climatic changes throughout the Holocene and the roles of solar forcing and natural variability in driving multidecadal, centennial, and millennial climatic behavior; some have focused on more recent periods or particular regions of the world (see, e.g., Bond et al. 2001; Christiansen and Ljungqvist 2012; Zhou and Tung 2013; Scafetta 2013; Wyatt and Curry 2014; Chylek et al. 2014a,b).

At the same time, attribution studies of recent global warming clearly show that anthropogenic forcings, and especially greenhouse gases (GHGs), are the main causes (Hegerl et al. 2007; Hegerl and Zwiers 2011). Other studies (Hoerling et al. 2008; DelSole et al. 2011) suggest that El Niño–Southern Oscillation (ENSO) and other circulation patterns of the coupled atmosphere–ocean system can influence the evolution of temperature behavior, over interannual to multidecadal time ranges. Furthermore, an interesting field of investigation is the study of how these influences on temperature changes can be combined in order to obtain reliable predictions of global temperature T for the next decades (Keenlyside et al. 2008).

Nearly 40 years ago (Manabe and Wetherland 1975), modeling studies began to show that augmented emissions of carbon dioxide are able to increase the global temperature. Since then, many attribution studies—until the updated synthesis in the last Intergovernmental

Corresponding author address: Antonello Pasini, CNR, Institute of Atmospheric Pollution Research, via Salaria km 29.300, I-00015 Monterotondo Stazione, Rome, Italy.
E-mail: pasini@iia.cnr.it

DOI: 10.1175/JCLI-D-13-00784.1

Panel on Climate Change (IPCC) report in 2013—found that anthropogenic activities (and especially GHG emissions) were the main cause of recent global warming. In the meantime, increasing evidence has been found of the influence of sea surface temperature (SST), mainly driven by coupled atmosphere–ocean oscillations, on the thermal variability of the climate system. The generally accepted view is that GHGs determine the recent trend in global temperature, while circulation patterns modify the behavior of T from year to year or even for as long as a few decades: see, for instance, Easterling and Wehner (2009). The above causal framework is taken for granted in the present study, even if we are aware that other opinions exist (see, e.g., Scafetta 2013).

In this framework of well-assessed factors of influence/cause on temperature behavior, here a specific analysis is performed in order to understand the relative strengths of these factors, and how they act on T. In particular, we show that analyzing the results of simple vector autoregressive models (VARs) for temperature prediction can clarify the individual roles of GHGs and ENSO in influencing recent temperature behavior.

We follow the same rationale used in correlation analyses when, if a well-established causality relationship between variables exists, they give information regarding the strength of that relationship. In particular, we adopt prediction models whose use has been shown to supply important causal information in attribution studies (Attanasio et al. 2012; Pasini et al. 2012). Even if we are aware that predictability is a necessary (but not sufficient) condition for causality, in cases of well-assessed influences such as those considered here we are confident that a deeper insight can be achieved through analyses such as the one described here.

The Atlantic multidecadal oscillation (AMO), the Pacific decadal oscillation (PDO), and other circulation patterns that exhibit a multidecadal period of oscillation are not considered here as this study concentrates on the behavior of T over two or three decades (see section 4). Thus, only ENSO, which exhibits an interannual to decadal oscillation, has been considered. Of course, the investigation could be extended in the future to cover other periods and/or circulation patterns.

It should be stressed that our approach is different from that of other empirical investigations of the relations between influence factors and temperature. In the past, some authors have dealt with the problem of the weighting of several influences on the recent global temperature time series by means of multilinear regressions (see, e.g., Lean and Rind 2008; Lean 2010; Foster and Rahmstorf 2011). This led to the development of empirical models that allowed the identification of the components of temperature variability due to various factors in in-sample investigations.

Here, instead, the focus is on the predictive capabilities of GHGs and ENSO and the use of empirical forecast models (to be tested out of sample), which are able to provide information about the relative importance of these specific influences. In particular, we show using predictive tests that the general accepted view (that GHGs determine the long-range behavior, and that ENSO contributes essentially to interannual and decadal variability) needs to be reconsidered, at least partially.

The data and methods used are described in sections 2 and 3, and the results obtained by application of VARs are presented in section 4. Brief conclusions are drawn in the final section.

2. Data

Our analysis is performed at global and hemispheric scales over the period 1866–2011. As far as temperatures are concerned, we adopt the annual data from version 4 of the Hadley Centre/Climatic Research Unit combined land and marine surface temperature global and hemispheric anomalies (HadCRUT4; Morice et al. 2012) (see Fig. 1). (Data are available online at http://www.cru.uea.ac.uk/data/.)

For GHGs, we consider annual CO_2, methane (CH_4), and nitrous oxide (N_2O) concentrations (Hansen et al. 2007; data available at http://data.giss.nasa.gov); we calculate radiative forcings (RFs) as in Ramaswamy et al. (2001) and consider a main GHG (CO_2 + CH_4 + N_2O) RF (hereafter GHG-RF) as the main external anthropogenic forcing (see Fig. 2). We use GHG-RF as a surrogate of the total anthropogenic forcing because of the common dependence (and high correlations) between the various anthropogenic effects, due to their mutual dependence on global economic activity, as shown in Lovejoy (2014), who used a similar surrogate.

Finally, in order to concisely describe the influence of ENSO, we consider annual data for the Southern Oscillation index (SOI; Ropelewski and Jones 1987; Allan et al. 1991; Können et al. 1998) (see Fig. 3). (Data are available online at www.cru.uea.ac.uk/cru/data/soi/soi.dat.)

3. Methods

In this study VARs are adopted. A VAR is a system of equations where current values of each variable depend on past values of the variable itself, past values of the other variables, and an error term. This model can be considered the natural extension of a univariate autoregressive model to a multivariate setting. Here we use bivariate VARs, that is,

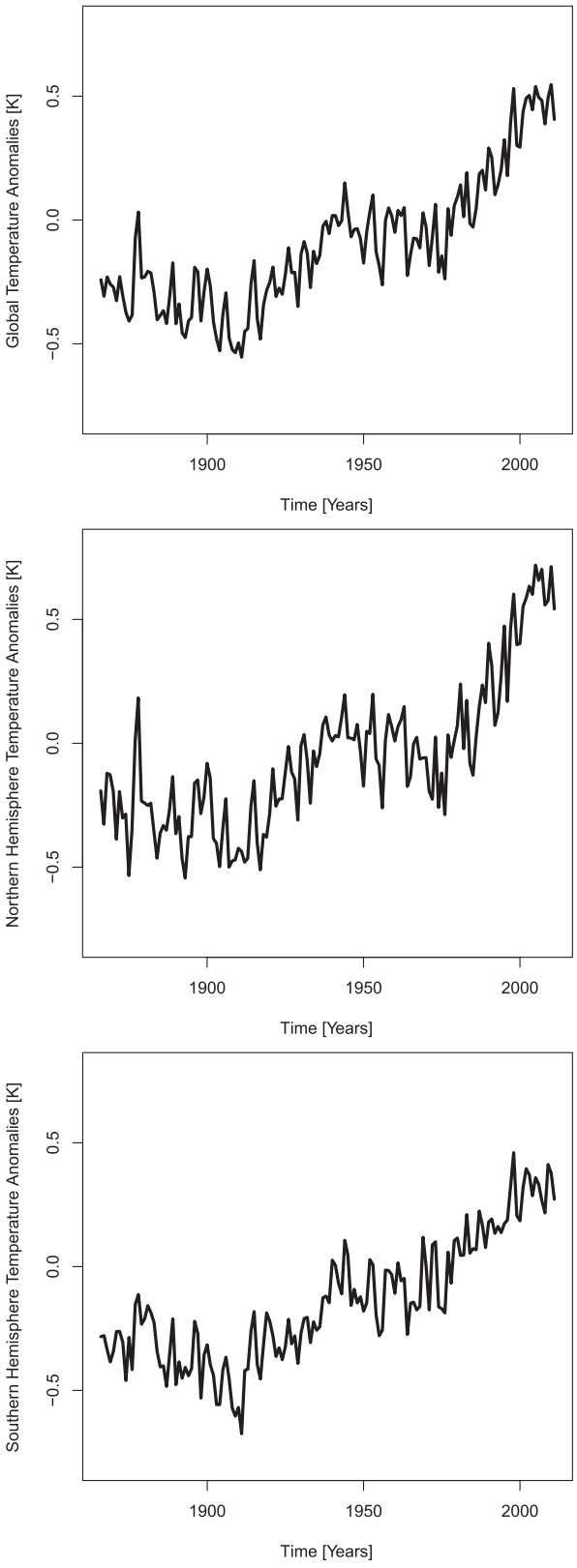

FIG. 1. Time series of temperature anomalies: (top) global, (middle) NH, and (bottom) SH.

$$x_t = a_1 x_{t-1} + \cdots + a_p x_{t-p} + b_1 y_{t-1} + \cdots + b_p y_{t-p} + e_t^x$$

and

$$y_t = c_1 x_{t-1} + \cdots + c_k x_{t-p} + d_1 m_{t-1} + \cdots + d_p m_{t-p} + e_t^y, \quad (1)$$

where e_t^x and e_t^y are random disturbances.

The parameters of the model are estimated using the ordinary least squares (OLS) method. The most common approach for model order selection involves selecting a model order that minimizes one or more information criteria, evaluated over a range of model orders. In this paper the Bayesian information criterion (BIC) is adopted (Lütkepohl 2005):

$$\mathrm{BIC}(p) = \ln|\tilde{\Sigma}| + \frac{K^2 p \ln T}{T}, \quad (2)$$

where $K = 2$ and $\tilde{\Sigma}$ is the maximum likelihood estimate of the covariance matrix of the disturbances in the VAR. In the literature other criteria have been proposed. The key difference among the criteria is how severely each one penalizes increases in model order (the second term in the above formula).

In general, we consider a vector y_t of possibly nonstationary (integrated of order d, $d = 1, 2$) variables, in order to specify a VAR for y_t.[1] We can utilize three different representations:

1) a VAR in levels (without any checking of stationarity),
2) a difference VAR (ensuring stationarity but not cointegration), and
3) a cointegrated VAR [a vector error-correction model (VECM) ensuring both stationarity and cointegration].

It has been argued (Sims et al. 1990) that a VAR in levels can be consistently estimated, independently of the order of integration of the series. On the other hand, it has also been shown that, in the presence of cointegration, there is a gain of efficiency if a VECM is used. However, it is important to note that the use of a VECM imposing incorrect cointegration restrictions (on the parameters) leads to inconsistent estimates. Estimating the VAR in levels avoids the possibility of imposing false restrictions on the model. For this reason we use VARs in levels rather than cointegrated VARs.

Three (real time) forecast exercises have been used in this study. We assume that the bivariate time series (x, y) follows a VAR of order p. We consider the problem of

[1] It is worthwhile to note, however, that there are some studies that show that temperatures are fractionally integrated (see, e.g., Gil-Alana 2003, 2005).

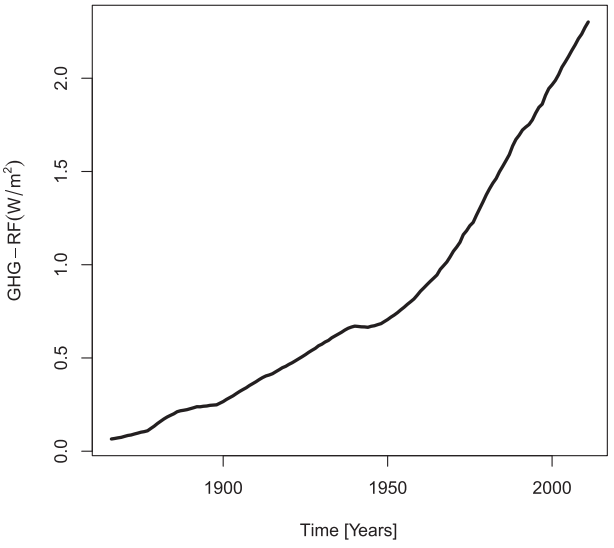

FIG. 2. Radiative forcing due to the three main GHGs.

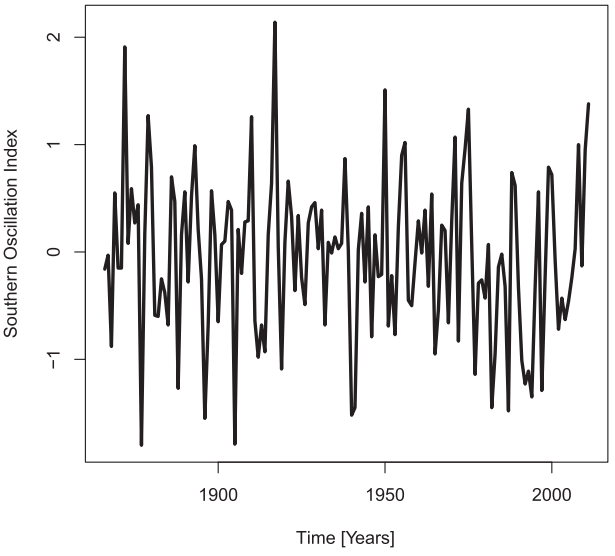

FIG. 3. Time series of the SOI.

forecasting the time series x, h periods into the future, given the information available at time t. The h-step ahead predictor is denoted by $\hat{x}_{t+h|t}$.

We use a direct forecast method, as follows:

- First, we estimate the projection equation

$$x_t = \alpha_1 x_{t-h} + \cdots + \alpha_p x_{t-h-p+1} + \beta_1 y_{t-h} + \cdots + \beta_p y_{t-h-p+1} + u_t^x. \quad (3)$$

- Then, using the estimated coefficients, the predictor $\hat{x}_{t+h|t}$ is obtained as

$$\hat{x}_{t+h|t} = \hat{\alpha}_1 x_t + \cdots + \hat{\alpha}_p x_{t-p+1} + \hat{\beta}_1 y_t + \cdots + \hat{\beta}_p y_{t-p+1}. \quad (4)$$

In the first forecast exercise the projection equations are estimated over the period 1866–1940 and $\hat{x}_{1940+h|1940}$ for $h = 1, 2, \ldots, 30$ are obtained. A new set of projection equations is estimated over the period 1866–1941 to obtain $\hat{x}_{1941+h|1941}$ for $h = 1, 2, \ldots, 30$, and so on up to 1981, when the last set of projection equations for the period 1866–1981 is estimated. In this way 42 forecasts for each horizon h are obtained. The forecasts concern the period 1941–2011.

Two further forecast exercises have been considered. In the second exercise the maximum forecast horizon is no longer 30 but 20. Thus the forecasts cover the period 1941–81. The third exercise considers the training period 1866–1970 and uses the estimated projection equations to obtain $\hat{x}_{1970+h|1970}$ for $h = 1, 2, \ldots, 20$, and so on. Here the forecasts concern the period 1971–2011. In these last two exercises the number of forecasts for each horizon h is 22.

In each forecast exercise, the model's performance is evaluated by calculation of the forecast mean square error (MSE). To assess the statistical significance of the differences between the MSEs obtained, we adopt the so-called Diebold–Mariano (DM) test (see Diebold and Mariano 1995). Let x_t denote the series to be forecast and let $x_{1,t+h|t}$ and $x_{2,t+h|t}$ denote two competing forecasts of x_{t+h} provided by two different models, model 1 and model 2, respectively. The forecast errors from the two models are

$$e_{1,t+h} = x_{t+h} - x_{1,t+h|t} \quad \text{and} \quad e_{2,t+h} = x_{t+h} - x_{2,t+h|t}. \quad (5)$$

The h-step forecasts are assumed to be calculated for $t = 1, 2, \ldots, n$ for a total of n forecasts giving $e_{1,1+h}, e_{1,2+h}, \ldots, e_{1,n+h}$ and $e_{2,1+h}, e_{2,2+h}, \ldots, e_{2,n+h}$. Thus a loss differential series $d_t = e^2_{1,t+h} - e^2_{2,t+h}$, $t = 1, 2, \ldots n$ can be constructed. The DM test statistic is a standard t ratio for testing the null hypothesis $H_0: d_t = 0$ of equal predictive accuracy between model 1 and model 2.

4. Results

To summarize, two VARs have been developed to test the performance of radiative forcing (GHG-RF, due to the three main greenhouse gases, $CO_2 + CH_4 + N_2O$) or ENSO (our y variable) in forecasting temperatures (our x variable) at both global and hemispheric scales. The first model (GHG-RF-T) is fed by temperature anomalies and GHG-RF data, and the second (SOI-T) is fed by temperature anomalies and SOI data. It should be stressed that two simple bivariate VARs are used not

because it is considered that GHGs and ENSO are independent influences on T, but rather because the aim is to compare their predictive abilities. The VARs are estimated in levels to avoid the possibility of imposing false restrictions on the models (Sims et al. 1990). The orders of the VARs are selected using the BIC (Diebold and Mariano 1995).

To avoid a dimensionality problem in our VARs (when the number of variables increase, VAR forecast performance deteriorates very fast), a number of influences on temperature considered in previous approaches, in particular solar forcing, are not included. As stated previously, the models used here include past temperature as a predicting variable. This permits the exclusion of this variable because it does not "cause" temperature in a Granger sense, as shown in Attanasio et al. (2012) and Pasini et al. (2012). In fact, it is well known that, if a variable y does not cause a variable x (T in this case), it implies that there is no additional information contained in the time series of y for the forecast of x in comparison with that included in the time series of x. In short, the time series of temperature accommodates these omitted influences. In any case, at the end of this section, the analysis has been extended to include the influence of volcanic forcing.

In this framework, as we will see, the analysis performed in the present paper permits the separate assessment of the roles of GHGs and ENSO in influencing future temperatures at global and hemispheric scales, and in distinct periods throughout the last 70 years.

In the first forecasting experiment, global temperatures are considered, the two models are trained using the period 1866–1940, and predictions are performed, via a direct method, for the test period 1941–2011 at annual forecast horizons $h = 1, \ldots, 30$. In this way 42 forecasts for each horizon were obtained. The results are summarized in Fig. 4, where the MSEs at each horizon are plotted. As can be seen, the SOI-T model errors increase steeply as the forecast horizon h increases, while the GHG-RF-T model shows only a slightly increasing trend with enhanced variability. These errors appear comparable until $h = 18$. After this forecast horizon, the GHG-RF-T model predictions appear more realistic. To quantify the statistical significance of the differences in the predictions, the DM test has been adopted, and shows that after $h = 21$ the difference is significant at a 5% level.

These results are not completely consistent with the commonly accepted idea of a purely short-range influence of ENSO on T: here we find that information about ENSO can be important also at medium range (about 20 yr), whereas over longer time scales information about GHG-RF is needed in order to obtain a reasonable prediction.

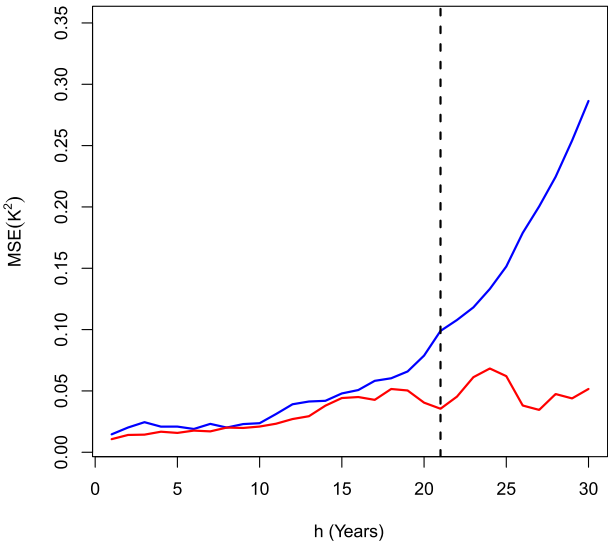

FIG. 4. Performance of our models shown in terms of forecast errors (MSE), GHG-RF-T model (red) and SOI-T model (blue); the dashed vertical line represents the forecast horizon where the performance of the models diverges significantly, according to the DM test.

It is worth noting that in this exercise the short-range forecasts concern a period with a quasi-stationary temperature trend, while, as h increases, the predictions refer to a period characterized by a steep increase in T (and in GHGs). Therefore, accordingly to this evidence, it is interesting to consider two subperiods (1941–81 and 1971–2011) that present different structural features: several studies recognized a structural break in the time series of global temperatures around 1976 (Mills 2013; Gay-Garcia et al. 2009). Using these two periods should test the whether the short- and medium-range influence of ENSO and long-range importance of GHGs are fixed features of the variables or if they are sensitive to the period considered. This new analysis gives a quite different picture (Fig. 5).

Here, in order to obtain an equal number of forecasts to be averaged for any h, only predictions up to $h = 20$ were considered. In the first period the performances of the two models are comparable and slightly worsen as the time horizon increases. We note that the forecasting performance of the SOI-T model is almost always better than that of the GHG-RF-T model. However, according to the DM test, their differences are never significant at the 5% level. This confirms the result presented previously. Conversely, in the second period, after the very first forecast horizons, the performances of the two models diverge greatly.

This clearly shows that the influences of GHGs and ENSO on T are equally important and persist in time during the period of quasi-stationary temperature

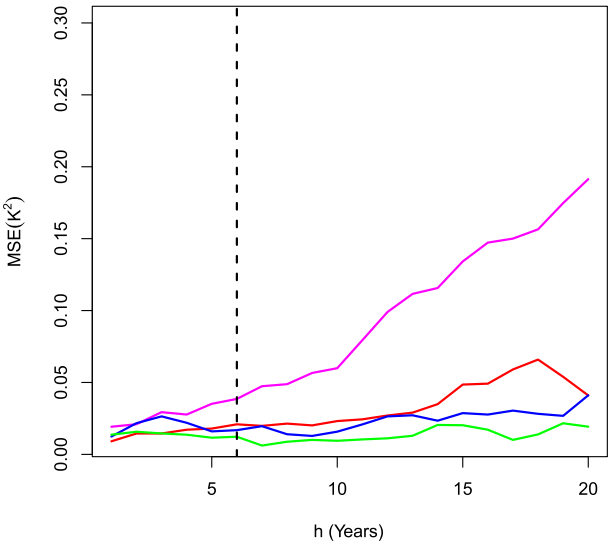

FIG. 5. Forecast errors of the two models (in terms of MSE) in the two periods considered: GHG-RF-T model 1941–81 (red line); SOI-T model 1941–81 (blue line); GHG-RF-T model 1971–2011 (green line); and SOI-T model 1971–2011 (magenta line). The vertical line shows the forecast horizon where the difference between model performances in the second period becomes significant at the 5% level.

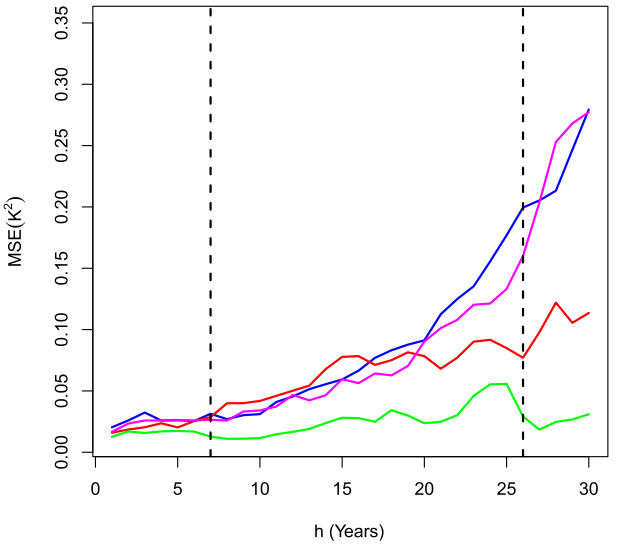

FIG. 6. Forecast errors of the two models (in terms of MSE) for the Northern and Southern Hemispheres: GHG-RF-T model NH (red line); SOI-T model NH (blue line); GHG-RF-T model SH (green line); and SOI-T model SH (magenta line). The vertical lines show the forecast horizons where the differences in model performance become significant at the 5% level.

behavior. On the other hand, in the period of increasing T the influence of ENSO persists only over a very short range and then is rapidly overwhelmed by the dominant role of GHGs.

Thus, the predictive ability of ENSO is sensitive to the dynamical evolution of the temperature time series. When the time series is characterized by a strong trend, ENSO shows poor predictive ability, whereas in stationary periods, when the cyclic component of the series becomes important, ENSO predictive ability is comparable to that of GHGs. Therefore, the crucial element for understanding the differing performance of ENSO is not the forecast horizon, but rather the absence or presence of a trend in T. It is worthwhile to note that this result is not a trivial one, because our predictive models do not regress T versus SOI only, but temperature is also an explicative variable which contains information on trends.

Thus a significant change in the influence role of ENSO on T is seen depending on the time periods considered. It is therefore worthwhile to investigate if similar changes can be found when different spatial domains (e.g., the two hemispheres) are considered.

At hemispheric scales (see Fig. 6), with reference to the results discussed for the global scale over the full period (1941–2011), the results show that in the Northern Hemisphere the performance of SOI-T model is generally comparable to that of GHG-RF-T model up to h = 25 (the differences are not significant at the 5% level), while over longer ranges the GHG-RF-T model performs better. For the Southern Hemisphere the results are comparable only up to h = 6, after which the model predictions diverge significantly.

These hemispheric results also show (Fig. 6) that the predictive abilities of ENSO are quite similar in the two hemispheres. As far as the role of GHGs is concerned, we find that the GHG-RF-T model performance is better in the Southern Hemisphere. This could be considered in contrast with the generally accepted view of a more significant influence from GHGs at northern high latitudes and over land. In this case, the better forecast performance of GHGs in the Southern Hemisphere should not be interpreted to mean that their role is greater here. We suggest that the increased predictability in the Southern Hemisphere is due to the smoother (i.e., more persistent) temperature time series, as a result of the dominant influence of the oceans. This can be shown by simple calculation of the autocorrelation functions, or by the persistence analysis of hemispheric time series performed in Triacca et al. (2014). Furthermore, in the Northern Hemisphere, the GHG-RF-T model performance probably suffers because of the presence of enhanced interannual oscillations in T.

During the first subperiod, 1941–81, at hemispheric scales (Fig. 7) we note that the performance of the SOI-T model does not substantially depend on the hemisphere considered, while the GHG-RF-T model gives better results for the Southern Hemisphere. When the second

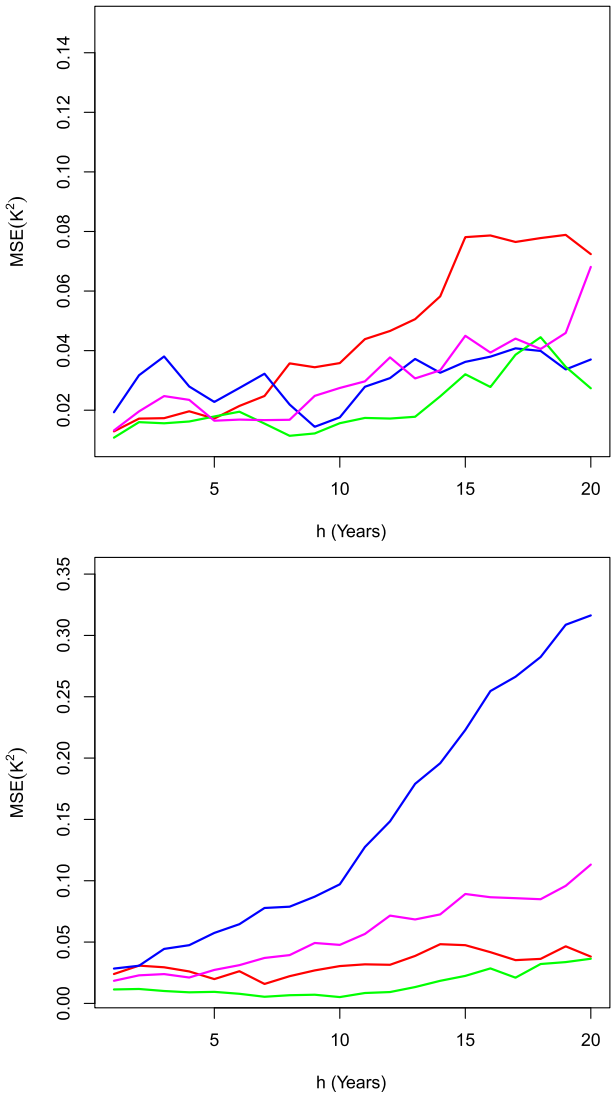

FIG. 7. Forecast errors of the two models (in terms of MSE) for NH and SH in two distinct periods, (top) 1941–81 and (bottom) 1971–2011: GHG-RF-T model NH (red line); SOI-T model NH (blue line); GHG-RF-T model SH (green line); and SOI-T model SH (magenta line).

period, 1971–2011, is considered, there is a clear evidence of a worsening in the SOI-T model performance in the Northern Hemisphere after $h = 10$.

To test the robustness of the results, volcanic forcing was included as a context variable in trivariate VARs. However after including volcanic forcing, the roles of GHGs and ENSO do not change substantially, whichever temporal or spatial domain was considered. These results are available on request by authors.

Finally, it is important to underline the inferential nature of the results. The comparison of the MSEs for the different models is based on a statistical (DM) test that allows the evaluation of the differences to ascertain whether they are significant or not. To evaluate the robustness of the results from the statistical tests, the bootstrap-based test of Ashley (1998) was also used. The results obtained were very similar.

5. Conclusions

The results presented here are, in part, not consistent with the idea of ENSO as a purely short-range driver of interannual variability in T, and give a deeper insight in its role. In particular, we discover that the crucial element for understanding the differing performance of ENSO as a predictor is not the forecast horizon, but the absence or presence of a trend in T. It is worthwhile to note that this is not a trivial result, because, even if ENSO does not exhibit a trend, the presence of the delayed values of T in Eq. (3) allows the effect of the trend to be removed. Thus, in principle, there is no reason to maintain that in a period of steeply increasing T, ENSO should provide a worse predictive performance than GHGs.

While the choice of different spatial domains (the two hemispheres) does not lead to substantial new results, the consideration of two time intervals—endowed with distinct structural features within the temperature time series—leads to the identification of a change in the role of ENSO linked to these features.

Summing up, ENSO short-range action is confirmed only for the recent period of steeply increasing temperature, while in the previous quasi-stationary period we find its role is very similar to that of GHGs, as far as both strength and time range of their influences are concerned. This suggests that ENSO lost its medium-range role in the most recent decades because of the overwhelming influence of GHGs, and that in other situations we can expect it to have an enhanced role. In this framework, further investigations are needed in order to understand if this will be the case if the recent hiatus in temperatures (Guemas et al. 2013) should persist into the near future. The predictive ability of GHGs is most evident in the Southern Hemisphere, where the temperature series is smoother.

Acknowledgments. We thank I. M. Hedgecock for helpful discussions.

REFERENCES

Allan, R. J., and Coauthors, 1991: A further extension of the Tahiti-Darwin SOI, early SOI results, and Darwin pressure. *J. Climate,* **4,** 743–749, doi:10.1175/1520-0442(1991)004<0743:AFEOTT>2.0.CO;2.

Ashley, R., 1998: A new technique for postsample model selection and validation. *J. Econ. Dyn. Control,* **22,** 647–665, doi:10.1016/S0165-1889(97)00085-7.

Attanasio, A., A. Pasini, and U. Triacca, 2012: A contribution to attribution of recent global warming by out-of-sample Granger causality analysis. *Atmos. Sci. Lett.,* **13,** 67–72, doi:10.1002/asl.365.

Bond, G., and Coauthors, 2001: Persistent solar influence on North Atlantic climate during the Holocene. *Science,* **294,** 2130–2136, doi:10.1126/science.1065680.

Christiansen, B., and F. C. Ljungqvist, 2012: The extra-tropical Northern Hemisphere temperature in the last two millennia: Reconstructions of low-frequency variability. *Climate Past,* **8,** 765–786, doi:10.5194/cp-8-765-2012.

Chylek, P., M. K. Dubey, G. Lesins, J. Li, and N. Hengartner, 2014a: Imprint of the Atlantic multi-decadal oscillation and Pacific decadal oscillation on southwestern US climate: Past, present, and future. *Climate Dyn.,* **43,** 119–129, doi:10.1007/s00382-013-1933-3.

——, N. Hengartner, G. Lesins, J. D. Klett, O. Humlum, M. Wyatt, and M. K. Dubey, 2014b: Isolating the anthropogenic component of Arctic warming. *Geophys. Res. Lett.,* **41,** 3569–3576, doi:10.1002/2014GL060184.

DelSole, T., M. K. Tippett, and J. A. Shukla, 2011: A significant component of unforced multidecadal variability in the recent acceleration of global warming. *J. Climate,* **24,** 909–926, doi:10.1175/2010JCLI3659.1.

Diebold, F. X., and R. S. Mariano, 1995: Comparing predictive accuracy. *J. Bus. Econ. Stat.,* **13,** 253–263.

Easterling, D. R., and M. F. Wehner, 2009: Is the climate warming or cooling? *Geophys. Res. Lett.,* **36,** L08706, doi:10.1029/2009GL037810.

Foster, G., and S. Rahmstorf, 2011: Global temperature evolution 1979–2010. *Environ. Res. Lett.,* **6,** 044022, doi:10.1088/1748-9326/6/4/044022.

Gay-Garcia, C., F. Estrada, and A. Sánchez, 2009: Global and hemispheric temperatures revisited. *Climatic Change,* **94,** 333–349, doi:10.1007/s10584-008-9524-8.

Gil-Alana, L. A., 2003: An application of fractional integration to a long temperature series. *Int. J. Climatol.,* **23,** 1699–1710, doi:10.1002/joc.968.

——, 2005: Statistical modeling of the temperatures in the Northern Hemisphere using fractional integration techniques. *J. Climate,* **18,** 5357–5369, doi:10.1175/JCLI3543.1.

Guemas, V., F. J. Doblas-Reyes, I. Andreu-Burillo, and M. Asif, 2013: Retrospective prediction of the global warming slowdown in the past decade. *Nat. Climate Change,* **3,** 649–653, doi:10.1038/nclimate1863.

Hansen, J., and Coauthors, 2007: Climate simulations for 1880–2003 with GISS model E. *Climate Dyn.,* **29,** 661–696, doi:10.1007/s00382-007-0255-8.

Hegerl, G. C., and F. W. Zwiers, 2011: Use of models in detection and attribution of climate change. *Wiley Interdiscip. Rev.: Climate Change,* **2,** 570–591, doi:10.1002/wcc.121.

——, and Coauthors, 2007: Understanding and attributing climate change. *Climate Change 2007: The Physical Science Basis,* S. Solomon and Coauthors, Eds., Cambridge University Press, 663–745.

Hoerling, M., and Coauthors, 2008: What is causing the variability in global mean land temperature? *Geophys. Res. Lett.,* **35,** L23712, doi:10.1029/2008GL035984.

Keenlyside, N. S., M. Latif, J. Jungclaus, L. Kornblueh, and E. Roeckner, 2008: Advancing decadal-scale climate prediction in the North Atlantic sector. *Nature,* **453,** 84–88, doi:10.1038/nature06921.

Können, G. P., P. D. Jones, M. H. Kaltofen, and R. J. Allan, 1998: Pre-1866 extensions of the southern oscillation index using early Indonesian and Tahitian meteorological readings. *J. Climate,* **11,** 2325–2339, doi:10.1175/1520-0442(1998)011<2325:PEOTSO>2.0.CO;2.

Lean, J. L., 2010: Cycles and trends in solar irradiance and climate. *Wiley Interdiscip. Rev.: Climate Change,* **1,** 111–122, 10.1002/wcc.18.

——, and D. H. Rind, 2008: How natural and anthropogenic influences alter global and regional surface temperatures: 1889 to 2006. *Geophys. Res. Lett.,* **35,** L18701, doi:10.1029/2008GL034864.

Lovejoy, S., 2014: Scaling fluctuation analysis and statistical hypothesis testing of anthropogenic warming. *Climate Dyn.,* **42,** 2339–2351, doi:10.1007/s00382-014-2128-2.

Lütkepohl, H., 2005: *New Introduction to Multiple Time Series Analysis.* Springer, 764 pp.

Manabe, S., and R. T. Wetherland, 1975: The effects of doubling the CO_2 concentrations on the climate of a general circulation model. *J. Atmos. Sci.,* **32,** 3–15, doi:10.1175/1520-0469(1975)032<0003:TEODTC>2.0.CO;2.

Mills, T. C., 2013: Breaks and unit roots in global and hemispheric temperatures: An updated analysis. *Climatic Change,* **118,** 745–755, doi:10.1007/s10584-012-0672-5.

Morice, C. P., J. J. Kennedy, N. A. Rayner, and P. D. Jones, 2012: Quantifying uncertainties in global and regional temperature change using an ensemble of observational estimates: The HadCRUT4 data set. *J. Geophys. Res.,* **117,** D08101, doi:10.1029/2011JD017187.

Pasini, A., U. Triacca, and A. Attanasio, 2012: Evidence of recent causal decoupling between solar radiation and global temperature. *Environ. Res. Lett.,* **7,** 034020, doi:10.1088/1748-9326/7/3/034020.

Ramaswamy, V., and Coauthors, 2001: Radiative forcing of climate change. *Climate Change 2001: The Scientific Basis,* J. T. Houghton et al., Eds., Cambridge University Press, 349–416.

Ropelewski, C. F., and P. D. Jones, 1987: An extension of the Tahiti–Darwin Southern Oscillation index. *Mon. Wea. Rev.,* **115,** 2161–2165, doi:10.1175/1520-0493(1987)115<2161:AEOTTS>2.0.CO;2.

Scafetta, N., 2013: Discussion on climate oscillations: CMIP5 general circulation models versus a semi-empirical harmonic model based on astronomical cycles. *Earth Sci. Rev.,* **126,** 321–357, doi:10.1016/j.earscirev.2013.08.008.

Sims, C., J. Stock, and M. Watson, 1990: Inference in linear time series models with some unit roots. *Econometrica,* **58,** 113–144, doi:10.2307/2938337.

Triacca, U., A. Pasini, and A. Attanasio, 2014: Measuring persistence in time series of temperature anomalies. *Theor. Appl. Climatol.,* doi:10.1007/s00704-013-1076-9, in press.

Wyatt, M. G., and J. A. Curry, 2014: Role for Eurasian Arctic shelf sea ice in a secularly varying hemispheric climate signal during the 20th century. *Climate Dyn.,* **42,** 2763-2782, doi:10.1007/s00382-013-1950-2.

Zhou, J., and K.-K. Tung, 2013: Deducing multidecadal anthropogenic global warming trends using multiple regression analysis. *J. Atmos. Sci.,* **70,** 3–8, doi:10.1175/JAS-D-12-0208.1.